

Comparison of Respiratory Triggering and Gating Techniques for the Removal of Respiratory Artifacts in MR Imaging¹

Respiratory movement degrades magnetic resonance (MR) images of the chest and abdomen by increasing noise through the production of "ghost" artifacts and by decreasing edge sharpness in moving structures. Respiratory gating, which limits data acquisition to end-expiration, is successful in restoring edge sharpness and reducing ghosts but increases imaging time two to three times, which limits its use to sequences with short repetition times (TRs). To overcome this limitation, an alternative technique, respiratory triggering, was developed, which triggers the acquisition of an MR section at a fixed point on the respiratory cycle. This technique restores edge sharpness and reduces ghosts, but unlike gating, it can be used to produce an image at any phase of the respiratory cycle. Triggering requires long TRs since the TR is limited to the respiratory period (TP) or one-half of TP, depending on whether the same section is triggered once or twice during a single respiratory cycle. Gating and triggering were evaluated and compared for single-section and multi-section imaging of both volunteers and patients. The authors conclude that when a chest or abdominal survey is required, triggering takes less time than gating if TRs are required that exceed one-fifth of TP.

Index terms: Abdomen, MR studies • Magnetic resonance (MR), technology • Thorax, MR studies

Radiology 1986; 160:803-810

MAGNETIC resonance (MR) imaging is a powerful imaging modality in visualizing lesions of the head, pelvis, and extremities. However, MR has been generally less successful compared with other techniques in imaging the upper abdomen and thorax, with the exception of the heart and other mediastinal structures (1-4). There is evidence (5) that the main cause of this inferior performance is respiratory movement. Muller et al. (4) compared MR imaging and computed tomography (CT) for their ability to demonstrate pulmonary nodules. They found that CT was superior to MR imaging when the pulmonary nodules were situated near the diaphragm, where respiratory motion is greatest.

The period of the respiratory cycle is approximately 4 seconds in healthy individuals. Because MR image collection takes 2-15 minutes, patient respiratory motion during this period causes problems in formation of the image. Effects of respiratory motion on imaging are twofold. First, there is an increase in image noise from "ghost" artifacts, which are multiple copies of the image superimposed on the primary image in the phase-encoding direction. Second, there is degradation of spatial resolution (spatial blurring) in the direction of movement.

Respiratory motion artifacts can be reduced through two approaches: (a) reducing the imaging time to enable breath-holding during the entire data acquisition, and (b) using the respiratory cycle to control the MR data collection process.

Two techniques have been investigated to reduce imaging time: driven equilibrium imaging (6) and echo planar imaging (7-9). The driven equilibrium technique forces spin relaxation by using special radio frequency (RF) pulses that reduce the time required for T1 relaxation, therefore allowing the use of short repetition times (TRs). This method maintains image contrast and reduces imaging time but not enough to allow breath-holding. Echo planar imaging can maintain contrast and resolution with a time savings by modulating the phase-encoding gradient during data acquisition. Unfortunately, the sampling rate must be increased to prevent aliasing (7), which increases the bandwidth and decreases the signal-to-noise ratio. At present, this technique can decrease imaging time by approximately a factor of 4 (9), which is not sufficient to allow breath-holding.

Many investigators of MR have used the respiratory cycle to control the collection of data. Bailes et al. (10) have suggested that artifacts could be reduced by altering the order of the phase-encoded projections with a technique called respiratory ordered phase encoding (ROPE). In this technique, the projections with relatively weak phase-encoding gradient are collected at functional residual capacity (FRC), and the projections with relatively strong phase-encoding gradient are collected toward the end of inspiration. This reduces the ghost artifacts but does not correct spatial blurring. Others have used respiratory gating techniques (11-14). The respiratory pattern is monitored, and then upper and lower gating thresh-

¹ From the Department of Nuclear Medicine, Research Institute, St. Joseph's Hospital, 268 Grosvenor Street, London, Ontario N6A 4V2, Canada (F.S.P., D.J.D., R.L.N.) and the Department of Biophysics, University of Western Ontario (C.E.L.). From the 1985 RSNA annual meeting. Received December 13, 1985; revision requested January 24, 1986, and received April 15; accepted May 9. This work was supported in part by a grant (MA-9467) from the Medical Research Council of Canada and a grant (01268) from the Ministry of Health of Ontario. **Address reprint requests to F.S.P.**

© RSNA, 1986

See also the article by Axel et al. (pp. 795-801) in this issue.

olds are calculated. Only when the MR pulse sequence occurs within this window are the data stored and used to reconstruct the final image. Gating reduces respiratory artifacts but increases the total acquisition time two to three times.

In another technique, respiratory triggering (15), the respiratory cycle is used to control the imaging process directly by triggering the MR pulse sequence at a specified level of the respiratory cycle. This is similar to the method used for cardiac triggering (16). Triggering has two major advantages over respiratory gating. No data are discarded because data are collected from all pulse sequences, and imaging can be performed at various points of the respiratory cycle (analogous to performing cardiac imaging at various stages of the cardiac cycle [17]). In this study, we compared respiratory triggering with gating.

MATERIALS AND METHODS

MR Imaging

All images were acquired using a resistive MR unit (Technicare; Cleveland) operating at 0.15 T. All images were made using a spin-echo (SE) technique with an echo time (TE) of 30 msec, a section thickness of 1 cm, two buffers per projection, and TRs varying from 500 to 5,800 msec.

In each figure legend associated with an MR image, these parameters are identified using accepted nomenclature (18). For example, an SE image with a TE of 30 msec and a TR of 500 msec is specified as SE 500/30.

Respiratory Transducer

MR groups that have investigated respiratory gating have used a number of different transducers to monitor the respiratory cycle. Some transducers that worked well on volunteers failed when used on patients because the transducers and associated instrumentation were uncomfortable or were not adaptable to the irregular breathing patterns often observed with anxious patients. The pneumotachograph used by Prato et al. (11) and the nasal thermistor used by Ehman et al. (13) were not tolerated well by patients. Ehman et al. (13), Runge et al. (12), and Groch et al. (14) found that a pneumatic belt, positioned around the patient's abdomen to monitor circumferential changes, was better tolerated by patients and produced reliable results.

We used a similar monitoring device, consisting of a pneumatic cuff placed around the abdomen and connected via a 10-m air tube to a pneumatic respiration pressure transducer (model DPRTB, Grass Instrument, Quincy, Mass.). The transducer's signal is proportional to the circum-

ferential changes of the body wall associated with breathing. For the work reported here, the pneumatic cuff was placed around the abdomen because, for healthy subjects in the supine position, 60% of respiratory volume change is attributable to abdominal muscle action (19). The respiratory signal was amplified, transmitted through a low-pass filter at 60 Hz, and digitized in a microcomputer for display and analysis.

One problem encountered with this method of respiratory monitoring was baseline drift, which could be caused by electronic components, changes in the patient's FRC, or movement of the cuff and temperature changes of the cuff air. A method was developed to determine the baseline so that a correction for baseline drift could be made. The respiratory signal was sampled and digitized at intervals of approximately 40 msec for ten respiratory cycles. This resulted in approximately 100 samples per respiratory cycle for healthy subjects. From these data, a frequency histogram, $H(v)$, of the digitized voltage values, v , was generated and analyzed to determine the baseline, B . If we assume N samples were taken, then B was calculated as the average value of the digitized points in the lower region of the histogram:

$$B = \frac{\sum[H(v) \cdot v]}{\sum H(v)}, \quad (1)$$

when $0.08N < \sum H(v) < 0.20N$.

The lower 8.0% and the upper 80.0% of the data were excluded from the calculation. The lowest 8.0% of the digitized points in the histogram are not included because they account for unusually low voltage values caused by patient irregularities, such as coughs, which result in lung volumes below FRC. The upper 80.0% are not included because they account for lung volumes well above FRC. Both values were chosen experimentally by using healthy volunteers breathing quietly in the supine position. This calculation, which is done immediately following a trigger, takes approximately 0.5 seconds with our software. Therefore, it is usually completed before the next trigger point occurs and results in little increase in imaging time. This process was repeated throughout the study at intervals of ten respiratory cycles (about 40 seconds) so that the baseline was always known. All respiratory gating and triggering levels were set with respect to the calculated baseline. Therefore, these levels were independent of the baseline drift of the signal. For patients with irregular breathing cycles, the short-term fluctuations of the patient's respiratory baseline must not be included in the baseline correction. This was done by increasing the number of respiratory cycles used to calculate the baseline from ten to 16 cycles.

Respiratory Gating

The respiratory gating scheme is illustrated in Figure 1. Upper and lower gating thresholds, which were under opera-

tor control, were calculated from the respiratory cycle. For our images, the thresholds were set at 20% of the tidal volume (maximum minus baseline), centered about the baseline. The TR in this example was 500 msec (Fig. 1b). The MR data were gated into the MR computer only when the respiratory cycle was between the programmable thresholds (Fig. 1c). Therefore, the imaging time was increased two to three times because most of the respiratory cycle is outside of these thresholds.

Respiratory Triggering

In respiratory triggering (Fig. 1), the trigger level can be set at any specified fraction of the tidal volume above the baseline (Fig. 1a). When the respiratory signal passed through this level during inspiration, the MR pulse sequence was triggered, as indicated by the vertical solid lines in Figure 1d. Triggering was also done during expiration (vertical dashed lines in Fig. 1d). In both cases, the TR is the same as the period of the respiratory cycle, which is approximately 4 seconds. Because such TRs are approximately twice those that are routinely used in MR imaging, triggering was also done during both inspiration and expiration, which reduced the TR to approximately 2 seconds.

Phantom Studies

Experiments with phantoms were undertaken to study the effects of movement on MR imaging (5, 20) and to assess some of the improvements attainable using respiratory gating and triggering. Respiratory motion was simulated using an apparatus that moved a phantom in simple harmonic motion parallel to the bore of the imaging magnet.

Spatial blurring in the images was evaluated by assessing the edge of a moving structure. A 3.8-cm thick, cylindrical phantom filled with propylene glycol was placed so that its flat surface, which was in the xy-plane, was perpendicular to the imaging section, which was in the zx-plane. The image was analyzed by taking an 8-mm wide rectangular region of interest with the long dimension of the region perpendicular to the flat edge of the phantom (i.e., in the z-direction). The signal intensity within this strip increased quickly in the transition zone between the background and the phantom. When the phantom was stationary, the transition zone encompassed only a few pixels; however, with movement of the phantom in the z-direction, this transition zone widened. To quantify this effect, the slope of the MR signal intensity within the transition zone was used as a measure of edge sharpness. This was measured for the following values of the amplitude of movement: 0.1, 0.2, 0.5, 1.0, and 2.0 cm.

In a second experiment, the movement of a 500-ml bottle of 100 μ M manganese chloride (T1 = 521 msec, a T1 value similar to that of abdominal tissues) was monitored using the pneumatic cuff so that

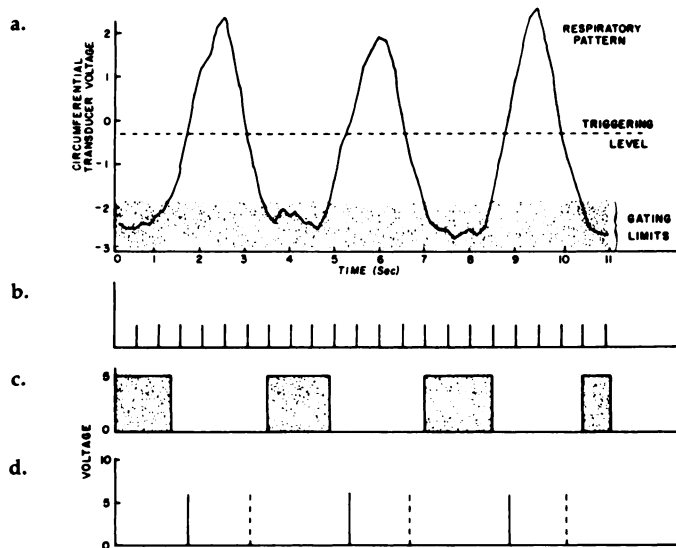


Figure 1. Schematic demonstrates the technique used for respiratory gated MR images and respiratory triggered MR images. (a) A typical respiratory signal with the gating limits shown by the shaded area centered about FRC and the triggering level shown by the horizontal, dashed line. (b) The vertical lines indicate the start of the imaging pulse sequence. In this example the TR is 500 msec. (c) The data are only acquired when the start of the pulse sequence falls within the gating limits, indicated by the shaded regions. (d) When the respiratory signal coincides with the trigger level during inspiration, the MR pulse sequence is started as indicated by the solid vertical lines. Similarly, triggering can occur during expiration (dashed vertical lines).

gating and triggering experiments could be performed. Transverse MR images of the phantom were obtained for control, gated, and triggered conditions. The direction of movement was perpendicular to the image plane.

Human Studies

Coronal images of young human volunteers, breathing quietly and spontaneously in the supine position, were obtained using respiratory gating and triggering techniques. To assess spatial blurring, the edge of the diaphragm was approximated as a moving edge, and the MR signal intensity was plotted perpendicular to the diaphragm. To test its feasibility as a valid triggering mode, images triggered during both inspiration and expiration (mode 3) were compared with images triggered only during inspiration (mode 1) and images triggered only during expiration (mode 2). To compare these images, the same TR had to be used for all three modes so that the contrast between tissues would be approximately constant. Therefore, when mode 3 was used, the MR imager was triggered only on every other respiratory cycle. Although this resulted in a TR that varied from 2 seconds to 6 seconds, experiments have shown that the averaging of the two data buffers per projection yields approximately the same recoverable signal intensity for phantoms, with T1 values representative of tissue (21). This is expected if the mean TR is significantly greater than the T1 of the imaged material.

RESULTS

Figure 2 is a graph of the slope of signal intensity perpendicular to the moving edge of the phantom filled with propylene glycol versus the amplitude of movement. This graph demonstrates that an amplitude greater than 2.0 mm caused significant degradation of the imaged edge of the phantom.

Figure 3 shows transverse images of the manganese chloride phantom in periodic motion (period = 4 seconds, approximately one breathing cycle) in and out of the image plane. Although there was no motion in the image plane, the control image (Fig. 3, upper right) has prominent ghost artifacts. The corresponding gated image (Fig. 3, upper left) demonstrates that the ghost artifacts were reduced by this technique but not completely removed. They were still produced because of the change in phantom position that occurs within the gating window. Gating may work better in clinical application because patients tend to have a prolonged period at end-expiration (Fig. 1a) that is not present in simple harmonic motion. The increase in imaging time was a factor of 2.5, which did not vary with TR. The lower left image in Figure 3 demonstrates the complete elimination of ghost artifacts by the

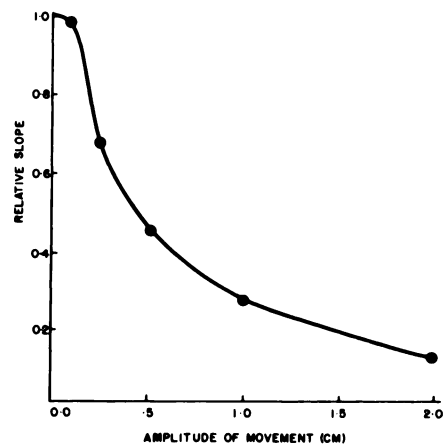


Figure 2. A plot of the slope of the change in MR signal intensity across the flat surface of a moving phantom filled with propylene glycol versus the amplitude of the phantom stroke.

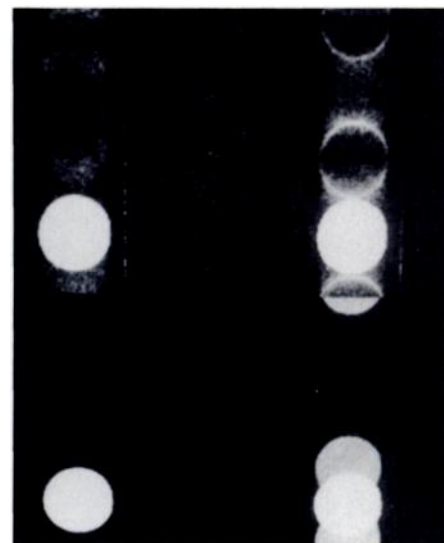


Figure 3. MR images of a 500-ml bottle of $MnCl_2$ (100 μM) that was moved sinusoidally, perpendicular to the image plane. The amplitude of motion was 2 cm, and the period was 4 second. The upper left image (SE 500/30) was gated with data acquisition restricted to a 2-mm range of phantom position. The image in the upper right (SE 500/30) was neither gated nor triggered and serves as a control for the gated image. The lower left image (SE 2,000/30) was triggered at a fixed position of the moving phantom. The lower right image (SE 2,000/30) was neither gated nor triggered and serves as a control for the triggered image.

triggering technique. Acquisition time was identical to the corresponding control image (Fig. 3, lower right). The ghost artifacts are absent because respiratory movement was removed by triggering at the same level during each respiratory cycle.

Coronal abdominal images in Figure 4 demonstrate the improvement in image quality achievable with respiratory gating. Fine structures with-

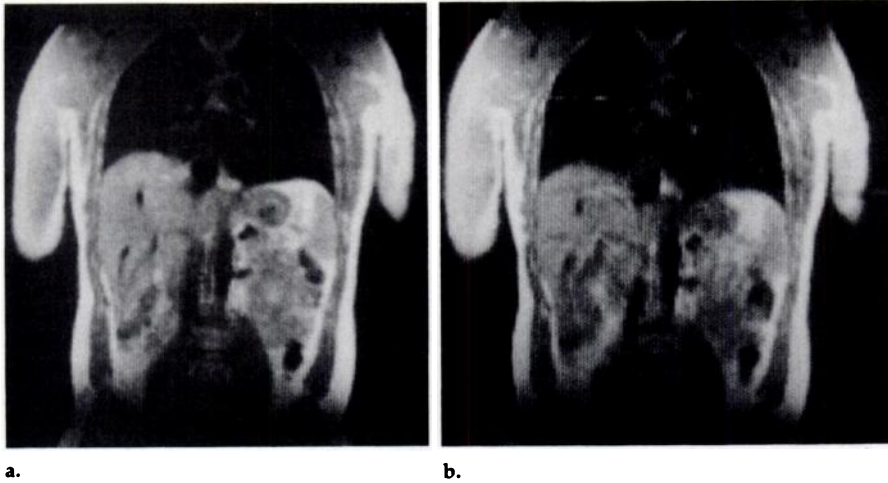


Figure 4. Coronal images of the abdomen of a healthy volunteer, breathing quietly in the supine position. (a) This image (SE 500/30) was respiratory gated at FRC. (b) This image (SE 500/30) was ungated and serves as a control for the gated image.

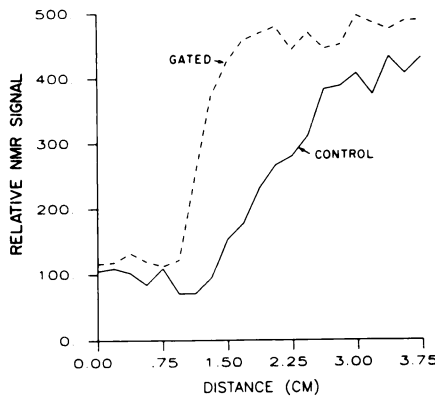


Figure 5. Plot of MR signal intensity measured from a 8-mm wide region perpendicular to the diaphragm for the respiratory gated (solid curve) and ungated (dashed curve) images of Fig. 4.

in the thorax and abdomen are more apparent in the respiratory gated image. Improvements in image quality were quantified by plotting the rate of change of signal intensity at the diaphragmatic edges of these two images (Fig. 5). Blurring of the diaphragmatic edge was significantly reduced, as indicated by the increased slope (edge definition) of the lung-diaphragm transition zone corresponding to the respiratory gated image.

In Figure 6, respiratory triggered images of a volunteer are compared with respiratory gated and control images. Two respiratory triggered images are shown in Figure 6, one triggered toward end inspiration (Fig. 6b), the other toward end-expiration (Fig. 6d). Acquisition times were identical to the control image. Respiratory triggered images showed improvements similar to those achieved by respiratory gating without increasing imaging time above

that required for untriggered images using comparable TRs (i.e., 4,000 msec). The diaphragmatic edges of the two triggered images plotted in Figure 7 are comparable to the respiratory gated edge (Fig. 5). By comparing the position of the diaphragmatic edges in Figure 7, we determined the diaphragmatic excursion, corresponding to about 80% of the tidal volume (inferred from the signal of the pneumatic cuff), to be 1.5 cm, which was consistent with values measured in healthy subjects with x-ray fluoroscopy (22).

In Figure 8 the diaphragmatic edges of four images are plotted: respiratory triggered only during inspiration (curve a), triggered only during expiration at the same level (curve b), triggered during both inspiration and expiration (curve c), and a control, untriggered condition (curve d). Figure 8 shows that respiratory triggering during both inspiration and expiration had no effect on the slope of the diaphragmatic edge or the position of the diaphragm, compared with the other two triggering modes.

DISCUSSION

The increase in systematic image noise associated with respiratory motion is a significant problem in obtaining MR images with good spatial resolution. The artifacts arise because respiratory motion adds a frequency modulation term to the Fourier transform in the phase-encoding direction. They are not propagated in the frequency-encoding direction because little time elapses during a single acquisition compared with the period of respiratory motion. How-

ever, the time between phase-encoded projections (TR) is of the order of the period of respiratory motion. Therefore, these artifacts are periodic in nature with a repeat distance (Y)—the vertical distance between adjacent artifacts—given by the following relationship (20):

$$Y = (2\pi F_m \cdot TR \cdot N_s) / (\gamma \Delta G \cdot T_y), \quad (2)$$

where F_m is the frequency of motion, TR is the repetition time, γ is the gyromagnetic ratio, ΔG is the phase-encoding gradient step, T_y is the phase-encoding gradient duration, and N_s is the number of buffers per projection. The intensity of the ghost artifacts increases as the amplitude of the motion increases. A method of reducing ghost artifacts is to choose TR using equation 2 so that the artifacts will occur beyond the image field of view (23). However, this method is not very flexible and does not reduce blurring.

In addition to the increase in imaging time (typically a factor of 2 to 3), respiratory gating did not totally remove the ghost artifacts because of the movement that is allowed. ROPE reduces ghost artifacts by making the variable of respiratory motion a monotonic function of the phase-encoding gradient strength (10). This causes F_m to approach zero so the quantity Y in equation 2 approaches zero. Respiratory triggering, however, completely eliminated the ghost artifacts because the MR data are collected at a virtually constant abdominal wall configuration ($F_m = 0$).

The second problem was the degradation of the image by the blurring of moving structures. Any imaging technique that collects data over several respiratory cycles is subject to image blurring because each projection will be distributed at a different point of the respiratory cycle. In fact, Figure 2 demonstrates that movement greater than 2.0 mm caused significant edge degradation, which is expected in an imaging modality with the resolution of 1–2 mm. The human diaphragm typically moves more than 2 cm during respiration (22). Therefore, lesions in the thorax and upper abdomen, particularly those adjacent to the diaphragm, are difficult to resolve (4).

ROPE does not reduce blurring because the MR data are acquired at random points of the respiratory cycle. Both respiratory gating and respiratory triggering restrict the data collection within a narrow range of abdominal wall configurations, and this reduces the blurring of moving

edges significantly. Figure 7 demonstrates another important advantage of respiratory triggering: imaging the same section at different lung volumes. Therefore, it would be possible to construct a cine-movie of the abdominal and thoracic contents during the respiratory cycle. This would have applications in studying the dynamics of respiration and in imaging organs and lesions that move with respiration.

Typical clinical MR imaging of the abdomen uses TRs on the order of 2,000 msec to image many sections. Because the TR is approximately four T1s (24), full T1 recovery is allowed, which increases the signal. Also, for best results, sections must be noncontiguous, otherwise there will be section interference, which results in loss of signal and contrast (25, 26).

There are two causes of section interference: (a) the RF section selection pulse excites protons in adjacent sections, and (b) tissue in the selected section moves during respiration into adjacent sections. The first factor can be reduced by defining the section more accurately using sinc RF pulses (27), but the second factor cannot be controlled unless imaging is synchronized with respiration. Section interference occurs even if all odd sections are excited first followed by the even sections since the time between section excitation would be of the order of two T1s. Therefore, for a complete body survey, two sets of multi-

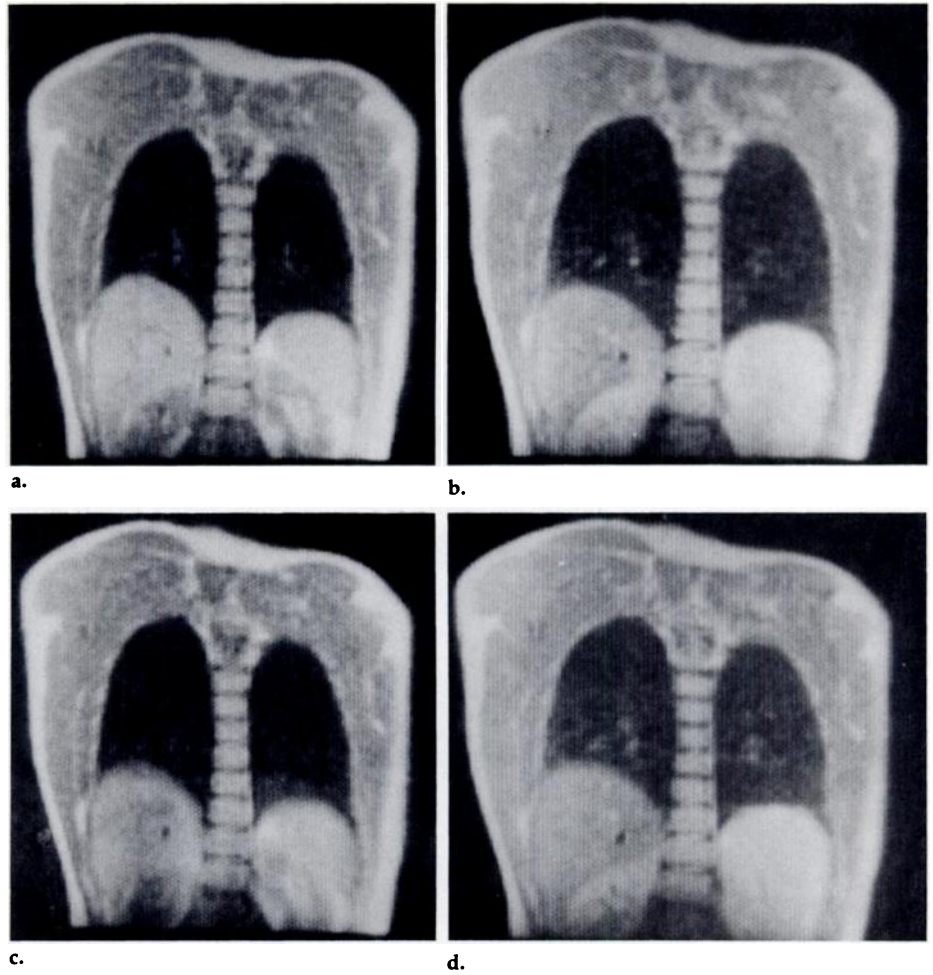
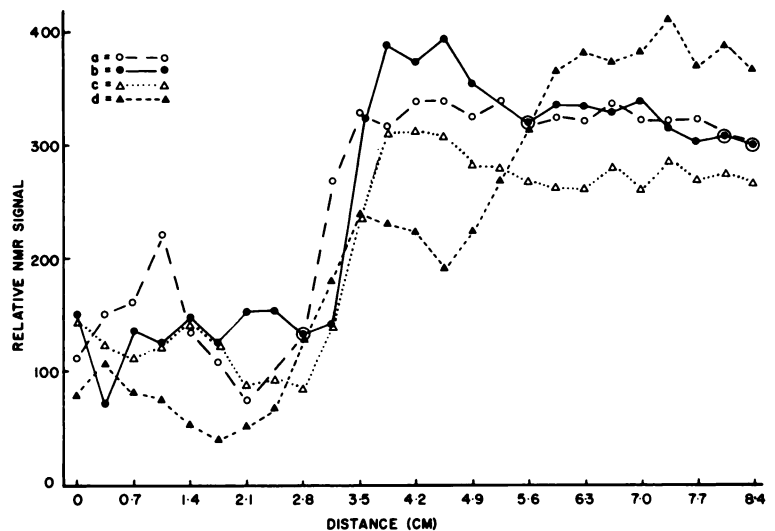
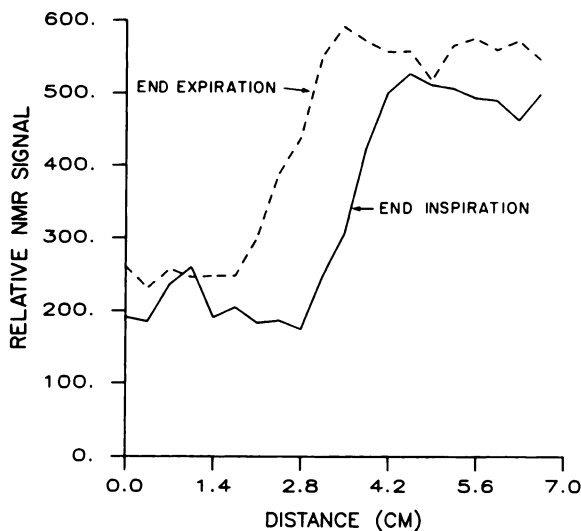


Figure 6. Coronal images of the chest and upper abdomen of a healthy volunteer, breathing quietly in the supine position. The image (SE 4,000/30) in **b** was respiratory triggered toward end inspiration. The image (SE 4,000/30) in **d** was respiratory triggered toward end-expiration, and the image (SE 500/30) in **a** was respiratory gated at FRC. The image (SE 500/30) in **c** was neither gated nor triggered.



Figures 7, 8. (7) Plot of signal intensity measured from an 8-mm wide region perpendicular to the diaphragm for the two respiratory triggered images of Fig. 6. The solid curve was triggered toward end inspiration, and the dashed curve was triggered toward end-expiration. (8) Plot of signal intensity for a 8-mm wide region perpendicular to the diaphragm. The images were obtained of a healthy volunteer breathing quietly in the supine position. *a* = SE 5,800/30 image respiratory triggered during inspiration, *b* = SE 5,800/30 image respiratory triggered during expiration, *c* = SE 5,800/30 image respiratory triggered during both inspiration and expiration (only every other respiratory cycle was used for triggering to obtain the same effective TR as the images represented by curves *a* and *b*), *d* = SE 5,800/30 untriggered image.

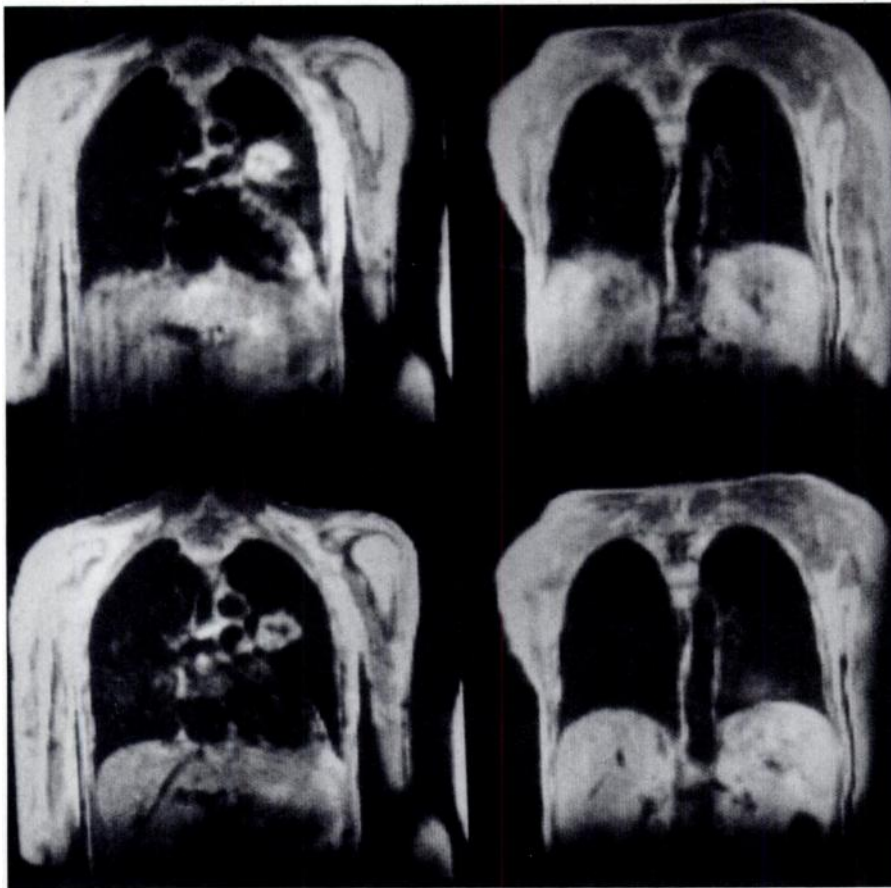


Figure 9. Respiratory triggered images on the bottom, with control images on the top, of a patient with bronchogenic carcinoma. The lower right image (SE 3,400/30) was the second section of a multisection sequence triggered during expiration. The lower left image (SE 3,400/30) was the fifth section of a multisection sequence triggered during inspiration. Both control images were obtained at SE 3,400/30.

section images with TRs of 2,000 msec must be collected so that the gaps of the first set are imaged.

Respiratory gating, for these long TRs, fails for two reasons: (a) the two-fold to threefold increase in imaging time becomes unacceptable, and (b) in multisection imaging, the later sections will not always occur within the gating thresholds because the data collection decision is made at the start of the pulse sequence, and this can occur just before an inspiration.

Respiratory triggering during inspiration only or expiration only requires the use of TRs that are equal to the period of the respiratory cycle (typically between 3.5 and 4.5 seconds), which is approximately twice the desired value. In multisection imaging, we can overcome this problem by collecting a contiguous set of images in which the odd sections are triggered during inspiration and the even sections during expiration. Two trigger levels are set: one during inspiration at 10% of tidal volume above FRC and the second during ex-

piration at 40% of tidal volume above FRC. The trigger during expiration starts the collection of odd sections, and the trigger during inspiration starts the collection of even sections, with all the sections having a TR equal to the mean respiratory period. Each even section is located between two odd sections and vice versa. For typical respiratory cycles, there is 1-2 seconds between the triggering of odd and even sections, which allows sufficient tissue relaxation before the interleaved sections are stimulated. Therefore, this technique allows contiguous chest and abdominal imaging, even for section overlap, without significant loss in image contrast caused by section interference.

In Figure 9 the triggered images of a patient with a bronchogenic carcinoma show improvement compared with the control images, particularly with respect to edge definition in the abdomen. In this technique, the sections triggered during expiration (odd-numbered) are approximately at the same lung volume (FRC), whereas the sections triggered during in-

spiration (even-numbered) occur at lung volumes that exceed FRC by at least 40% of tidal volume.

In situations in which only one set of sections needs to be collected, it is desirable to reduce the TR in respiratory triggering to one-half of the respiratory period. As we have shown (Fig. 8), this can be done for a single section by triggering at the same abdominal wall configuration during both inspiration and expiration. This is possible because changes in abdominal wall configuration during both inspiration and expiration are directly proportional to changes in position of the diaphragm and abdominal contents (28). Figure 10 shows images of a patient with metastatic spread to the lungs from a thymic carcinoma. These images clearly show pleural tumor at the left base immediately adjacent to the diaphragm. When the position of the diaphragm in the gated image, which was taken at FRC, was compared with the image triggered at 40% of tidal volume during both inspiration and expiration, the normal lung (right) showed an excursion of the diaphragm that was absent on the affected side (left). This suggested fibrosis in the diseased lung subsequent to chemotherapy, which was consistent with clinical findings.

This technique of monitoring abdominal circumference may be less successful for thoracic imaging because the abdominal component of respiration precedes lung volume changes during inspiration and lags lung volume changes during expiration (28). In fact, for upper thoracic imaging during both inspiration and expiration it may be necessary to move the circumferential transducer to the upper thorax or, if the transducer remains around the abdomen, to accept a small amount of blurring in the image. To extend respiratory triggering during both inspiration and expiration to multisection MR imaging, each section could be controlled independently and triggered at a separate voltage of the respiratory cycle. This technique would be useful in clinical abdominal imaging because it combines reasonable TRs with multisection capabilities. It would, however, require modification of conventional MR software to allow each section of a multisection sequence to be independently triggered.

The increase in imaging time for respiratory gating was compared with that of triggering (Fig. 11). The increase for gating was independent

of the TR used. Respiratory triggering during inspiration or expiration only is preferable to gating when TRs exceed approximately one-third to one-half of the respiratory period (TP) which corresponds to 1,500 msec in the case of Figure 11. However, when contiguous or overlapping sections are required for a complete tissue survey, triggering the odd and even sections separately is preferable when TRs exceed one-sixth to one-quarter of TP (approximately 750 msec in this case).

In summary, respiratory gating and triggering techniques were successful in reducing spatial blurring and eliminating the ghost artifacts. The respiratory gating technique worked well for TRs less than approximately 1,000 msec but was impractical for the longer TRs typically used in abdominal imaging. Respiratory triggering was successful for long TRs, and triggering the odd and even sections separately allows contiguous multisection imaging in a single acquisition with reduced section interference. Respiratory triggering can also be used to study the dynamics of respiration and associated movement of lesions and organs. We have demonstrated that respiratory triggering reduces respiratory artifacts, but a clinical trial is needed to determine the improvements that it offers in diagnosis. ■

Acknowledgments: We wish to thank Thomas Carr, M.D., George Yakemchuk, M.D., and Richard Knill, M.D., for clinical assistance and helpful comments and Todd Keys, M.Sc., for assistance with computer programming.

References

1. Didier D, Higgins CB, Fisher MR, Osaki L, Silverman NH, Cheitlin MD. Congenital heart disease: gated MR imaging in 72 patients. *Radiology* 1986; 158:227-235.
2. Stratemeier EJ, Thompson R, Brady TJ, et al. Ejection fraction determination by MR imaging: comparison with left ventricular angiography. *Radiology* 1986; 158:775-777.
3. Ross JS, O'Donovan PB, Novoa R, et al. Magnetic resonance of the chest: initial experience with imaging and in vivo T1 and T2 calculations. *Radiology* 1984; 152:95-101.
4. Muller NL, Gamsu G, Webb WR. Pulmonary nodules: detection using magnetic resonance and computed tomography. *Radiology* 1985; 155:687-690.
5. Schultz CL, Alfidi RJ, Nelson AD, Kapiwoda SY, Clampitt ME. Effect of motion on two-dimensional Fourier transformation magnetic resonance images. *Radiology* 1984; 152:117-121.
6. van Uijen CMJ, den Boef JH. Driven-equilibrium radiofrequency pulses in NMR imaging. *Magn Reson Med* 1984; 1:502-507.

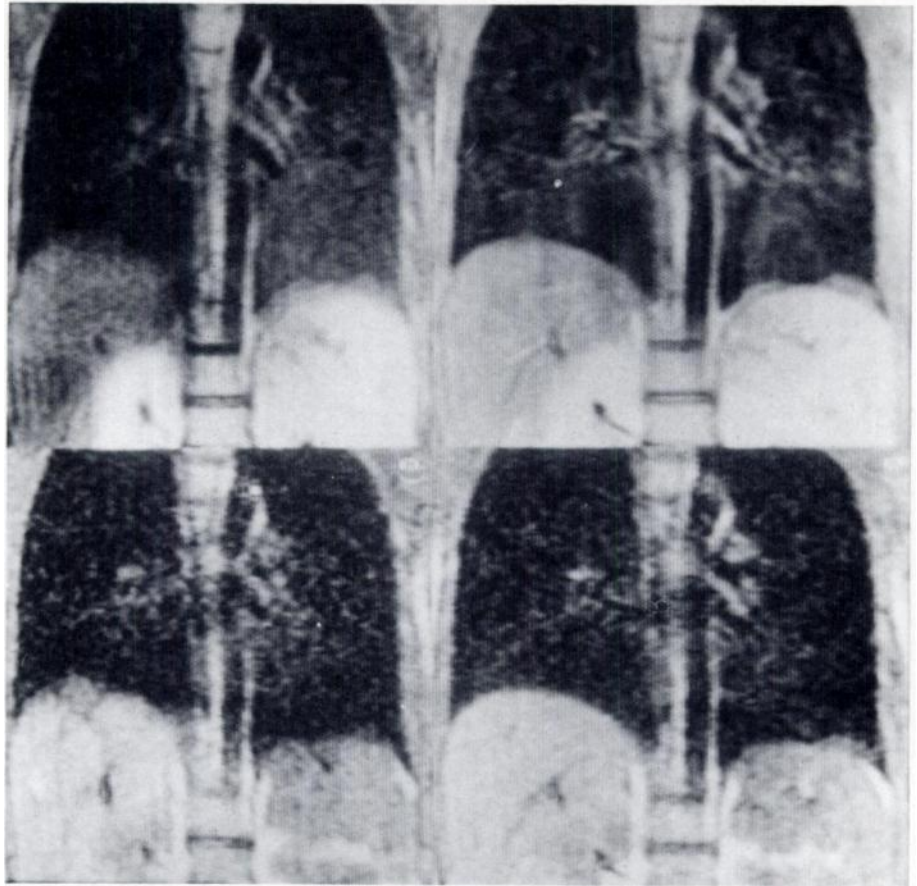


Figure 10. A 31-year-old woman with metastatic spread to her lungs from a primary cancer located in her thymus. The upper right (SE 2,000/30) image was triggered during both inspiration and expiration at 40% of tidal volume. The image on the lower right (SE 500/30) was gated at FRC. The upper left image (SE 2,000/60) was neither triggered nor gated. The image on the lower left (SE 500/30) was neither gated nor triggered and serves as control for the gated image.

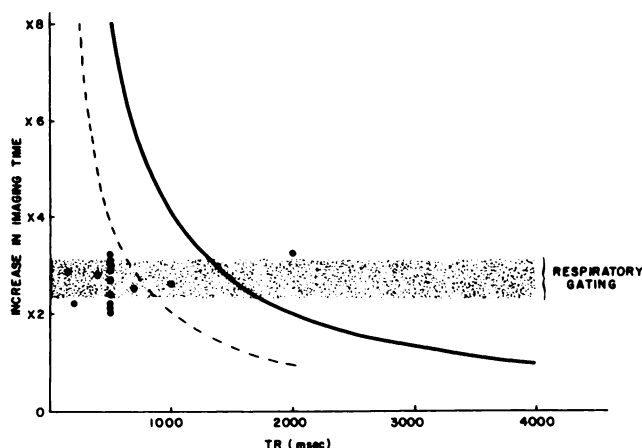


Figure 11. Increase in imaging time equal to the imaging time of a respiratory gated or triggered image divided by a control (neither gated nor triggered) image as a function of the control image TR. The increase associated with gating (shaded region) corresponds to mean increases (\pm standard deviation) experimentally measured for TR values ranging from 175 to 2,000 msec. The solid curve corresponds to the increase for respiratory triggering if TR is set equal to TP. The dashed curve corresponds to the increase for triggering if TR is set equal to one-half of TP or if two sets of control images must be acquired to be comparable to triggering the odd and even sections separately when contiguous or overlapping sections are needed.

7. Cuppen JJ, Groen JP. Improved method for MR fast Fourier imaging. *Radiology* 1984; 153(P):215.
8. van Uijen CMJ, den Boef JH, Verschuren FJJ. Fast Fourier imaging. *Magn Reson Med* 1985; 2:203-217.
9. Haacke EM, Bearden FH, Clayton JR, Linga NR. Reduction of MR imaging time by the hybrid fast-scan technique. *Radiology* 1986; 158:521-529.
10. Bailes DR, Gilderdale DJ, Bydder GM, Collins AC, Firmin DN. Respiratory ordered phase encoding (ROPE): a method for reducing respiratory motion artifacts in MR imaging. *J Comput Assist Tomogr* 1985; 9:835-838.
11. Prato FS, Nicholson RL, King M, Knill RL, Reese L, Wilkins K. Abolition of respiratory movement markedly improved NMR images of the thorax and upper abdomen. *Magn Reson Med* 1984; 1:227-229.
12. Runge VM, Clanton JA, Partain CL, James AE. Respiratory gating in magnetic resonance imaging at 0.5 tesla. *Radiology* 1984; 151:521-523.
13. Ehman RL, McNamara MT, Pallack M, Hricak H, Higgins CB. Magnetic resonance imaging with respiratory gating: techniques and advantages. *AJR* 1984; 143:1175-1182.
14. Groch MW, Turner DA, Clark JW. A respiratory gating device for MR imaging. *Radiology* 1984; 153(P):98.
15. Lewis CE, Prato FS, Drost DJ. Respiratory triggering removes artifacts from MR images without significant increase in imaging time. *Radiology* 1985; 157(P):204.
16. Lanzer P, Botvinick EH, Schiller NB, et al. Cardiac imaging using gated magnetic resonance. *Radiology* 1984; 150:121-127.
17. Chang W, Henkin RE, Hale DJ, Hall D. Methods for detection of left ventricular edges. *Semin Nucl Med* 1980; 10:39-53.
18. Commission on NMR for the American College of Radiology. *ACR NMR glossary*. Chevy Chase, Md.: American College of Radiology, 1983.
19. Sharp JT, Goldberg NB, Druz WS, Danon J. Relative contributions of rib cage and abdomen to breathing in normal subjects. *J Appl Physiol* 1975; 39:608-618.
20. Wood ML, Henkelman RM. MR image artifacts from periodic motion. *Med Phys* 1985; 12:143-151.
21. Galland C, Drost DJ, Prato FS, Wisenberg G. Tolerance limits on repetition times improve the precision in T1s calculated from cardiac triggered MRI images. Presented at the Fourth Annual Meeting of the Society of Magnetic Resonance in Medicine, London, England, August 19-23, 1985.
22. Froese AB, Bryan AC. Effects of anaesthesia and paralysis on diaphragmatic mechanics in man. *Anaesthesiology* 1974; 41:242-255.
23. Axel L, Charles C, Kressel H, Summers R, Kundel HL. Respiratory effects in two-dimensional Fourier transform MR imaging. *Radiology* 1985; 157(P):296.
24. Bottomley PA, Foster TH, Argersinger RE, Pfeifer LM. Review of normal tissue hydrogen NMR relaxation times and relaxation mechanisms from 1-100 MHz: dependence on tissue type, NMR frequency, temperature, species, excision, and age. *Med Phys* 1984; 11:425-448.
25. Fitzsimmons JR, Googe RE. Multisection-multiecho MR imaging: effect on image quality. *Radiology* 1985; 157:813-814.
26. Kneeland JB, Shimakawa A, Wehrli FW. Effect of intersection spacing on MR image contrast and study time. *Radiology* 1986; 158:819-822.
27. Feinberg DA, Crooks LE, Hoenninger JC, et al. Contiguous thin multisection MR imaging by two-dimensional Fourier transform techniques. *Radiology* 1986; 158:811-817.
28. Konno K, Mead J. Measurement of the separate volume changes of rib cage and abdomen during breathing. *J Appl Physiol* 1967; 22:407-422.